



**HAL**  
open science

## Pilot-scale biomethanation of cattle manure using dense membranes

Aline Lebranchu, Fabrice Blanchard, Michel Fick, Stéphane Pacaud, Eric Olmos, Stéphane Delaunay

► **To cite this version:**

Aline Lebranchu, Fabrice Blanchard, Michel Fick, Stéphane Pacaud, Eric Olmos, et al.. Pilot-scale biomethanation of cattle manure using dense membranes. *Bioresource Technology*, 2019, 284, pp.430-436. 10.1016/j.biortech.2019.03.140 . hal-02968858

**HAL Id: hal-02968858**

**<https://hal.science/hal-02968858>**

Submitted on 22 Oct 2021

**HAL** is a multi-disciplinary open access archive for the deposit and dissemination of scientific research documents, whether they are published or not. The documents may come from teaching and research institutions in France or abroad, or from public or private research centers.

L'archive ouverte pluridisciplinaire **HAL**, est destinée au dépôt et à la diffusion de documents scientifiques de niveau recherche, publiés ou non, émanant des établissements d'enseignement et de recherche français ou étrangers, des laboratoires publics ou privés.



Distributed under a Creative Commons Attribution - NonCommercial 4.0 International License

# Pilot-scale biomethanation of cattle manure using dense membranes

Aline LEBRANCHU<sup>a,b</sup>, Fabrice BLANCHARD<sup>a,b</sup>, Michel FICK<sup>a,b</sup>, Stéphane PACAUD<sup>c</sup>, Eric OLMOS<sup>a,b,\*</sup>, Stéphane DELAUNAY<sup>a,b</sup>

<sup>a</sup> CNRS, Laboratoire Réactions et Génie des Procédés, UMR 7274, 2 avenue de la forêt de Haye, TSA 40602, Vandœuvre-lès-Nancy, F-54518, France

<sup>b</sup> Université de Lorraine, LRGP, UMR 7274, 2 avenue de la forêt de Haye, TSA 40602, Vandœuvre-lès-Nancy, F-54518, France

<sup>c</sup> ENSAIA, Université de Lorraine, 2 avenue de la forêt de Haye, TSA 40602, Vandœuvre-lès-Nancy, F-54518, France.

---

## Abstract

This study aimed at studying the biomethanation process using a 100 L pilot-scale digester equipped with a dense membrane for hydrogen injection. Hydrogen mass transfer was characterized and the impact of hydrogen flowrate, agitation rate and of the co-injection of CO<sub>2</sub>, on biogas production and composition, was precisely studied. A linear relationship between H<sub>2</sub> flowrate and the CO<sub>2</sub> and CH<sub>4</sub> rates in biogas was found but no impact on biogas flowrate was shown. It was also noticed that, without exogenous CO<sub>2</sub> injection, and for high H<sub>2</sub> injection flowrates, residual H<sub>2</sub> could be found at the digester outlet due to local CO<sub>2</sub> limitation. Thus, this study suggested that biogas production in biomethanation process at the pilot scale was probably rather limited by the dissolved CO<sub>2</sub> transport within the liquid phase than by the hydrogen mass transfer itself.

*Keywords:* biomethanation, permeation membrane, pilot-scale digester, methanization

---

\*Corresponding author : [eric.olmos@univ-lorraine.fr](mailto:eric.olmos@univ-lorraine.fr)

1 **1. Introduction**

2 Anaerobic digestion is a natural biological process that transforms organic matter  
3 into biogas, consisting mainly of methane (about 60 %) and carbon dioxide (about  
4 40 %). This is today a widespread way of producing green energies and that may  
5 simultaneously allow the recovery of organic wastes. To increase the rate of methane  
6 in the biogas, one possibility is the injection of hydrogen into the digesters. In fact,  
7 the natural production of hydrogen transformed into methane by hydrogenotrophic  
8 methanogenic *Archae* ( $4\text{H}_2 + \text{CO}_2 \rightarrow \text{CH}_4 + 2\text{H}_2\text{O}$ ) is limiting. Thus, by inject-  
9 ing exogenous hydrogen, the hydrogenotrophic methanogenic *Archae* could consume  
10 more  $\text{CO}_2$  naturally produced in the reactor, and thus increase the rate of methane  
11 in biogas.

12 Injection of gaseous hydrogen to improve methanation reaction in digesters has  
13 been the subject of publications which demonstrated that several parameters may  
14 affect the efficiency of hydrogen injection, including the operating temperature and  
15 the mode of process performance. The main problem identified by Luo et al. (2012),  
16 Luo and Angelidaki (2012), Luo and Angelidaki (2013a) and Bassani et al. (2015)  
17 is indeed a problem of efficiency of hydrogen mass transfer in the reaction medium,  
18 leading to the presence of hydrogen in the biogas. These studies using different  
19 substrates (sludge STEP for Luo and Angelidaki (2012), bovine manure for Luo  
20 et al. (2012) and Luo and Angelidaki (2013a)) demonstrated the impact of some  
21 operating conditions on the effectiveness of the injection of hydrogen. These were  
22 the pressure of the  $\text{H}_2/\text{CO}_2$  mixture injected in the headspace of the reactor (Luo  
23 et al., 2012), the agitation rate (Luo et al., 2012; Luo and Angelidaki, 2012, 2013a)  
24 and the design of the gas supplier (Luo and Angelidaki, 2012, 2013a).

25 Luo and Angelidaki (2012) also showed that the amount of dissolved hydrogen

26 was very small regarding the amount of hydrogen that was expected by applying a  
27 mass balance on the gaseous hydrogen. With an injection of H<sub>2</sub> to 12 L/(L d) and  
28 an agitation rate of 500 rpm, the dissolved concentration of H<sub>2</sub> was indeed about 8  
29 μmol/L while the expected one was 45 μmol/L. The difference between these two  
30 values highlighted a limiting step of transfer from gas to liquid phase due to non-  
31 adapted hydrodynamic conditions.

32 To improve the absorption of hydrogen in the liquid phase, two strategies were con-  
33 sidered: the biogas recirculation and injection of hydrogen through membranes, in  
34 order to avoid the formation of bubbles and the loss of H<sub>2</sub> in the outlet gas phase.  
35 Biological methanation by recirculation of the biogas in the solution was proposed by  
36 Alfaro et al. (2019) and Kougiyas et al. (2017). Three configurations of digesters and  
37 different recirculation rates were compared by these last authors. Studied reactors  
38 were two columns in series, a Continuous Stirred Tank Reactor and a bubble column.  
39 The best results were achieved in the column reactors with the highest recirculation  
40 and flowrate reaching a consumption of up to 100 % H<sub>2</sub> and in the bubble column,  
41 with a rate of methane reaching 98 % in the biogas.

42  
43 In order to address the problem of hydrogen absorption, in several studies, pure  
44 hydrogen or hydrogen mixed with CO or CO<sub>2</sub> was injected by using permeation  
45 hollow fiber membranes. The membranes used were non-porous polyurethane mem-  
46 branes (Luo and Angelidaki, 2013b; Wang et al., 2013) or PVDF (polyvinylidene  
47 fluoride) (Díaz et al., 2015). Studies using non-porous membranes agreed on the fact  
48 that hydrogen was entirely consumed, since there was no hydrogen in the biogas.  
49 Methane rates above 96 % in biogas were reported (Ju et al., 2008; Luo and Angel-  
50 idaki, 2013b) which illustrated the effectiveness of an injection by permeation. The  
51 study of Díaz et al. (2015) also showed a very good efficiency in the consumption of

52 hydrogen, with more than 95 % of the  $H_2$  injected effectively consumed. However,  
53 it was found in this last study that, on the first days of digestion, a large part of  
54 the injected hydrogen was used for biomass growth, and not for the production of  
55 methane. Moreover, the development of a biofilm on the surface of the membrane  
56 was observed (Luo and Angelidaki, 2013b) and could increase the resistance of hy-  
57 drogen mass transfer. Apart from the study of Kim et al. (2013), carried out in a 100  
58 L reactor and considering an *ex-situ* culture of hydrogenotrophic *Archae*, the studies  
59 were conducted in low volumes laboratory-scale reactors.

60 In this study, biomethanation reaction was carried-out in a 100 L bioreactor, using a  
61 silicone permeation membrane, to assess the robustness of *in-situ* biomethanation at  
62 the pilot-scale. First, the permeation characteristics of the membrane and the gas-  
63 liquid mass transfer performance of this system were determined. Next, the impact  
64 of the shear rate and hydrogen flow rate on the biogas production and composi-  
65 tion were studied. Finally, the performance of methanation were determined using a  
66 co-injection of hydrogen and  $CO_2$ .

## 67 2. Materials and methods

### 68 2.1. Pilot-scale digester

69 The total volume of the tank was 142 L, with a diameter of  $D_{vessel} = 500$  mm  
70 and a height  $H = 760$  mm. The sketch of the bioreactor is reported on Figure 1. As  
71 demonstrated in a previous study (Lebranchu et al., 2017), the stirrer preferred was  
72 a double helical ribbon as it offered better mixing performance and allowed enhanced  
73 biogas productivity. This stirrer was combined here with a central Archimede's screw  
74 wrapped around the axis of agitation. Both systems were connected to an ATEX  
75 motor. The ribbon was sized in geometric similarity with the one previously used in

76 a 2 L digester as reported by Lebranchu et al. (2017). The pitch of the ribbon was  
77 500 mm, its width was 48 mm while its internal and external diameters were 384  
78 and 80 mm respectively. For the screw, the dimensions were a pitch of 298 mm, a  
79 blade width of 54 mm and an internal radius of 12 mm. The wrapping direction was  
80 opposite to that of the external ribbon. The agitator was also equipped with a Teflon  
81 scraper with a height of 35 mm to prevent the formation of crust at the bottom of  
82 the reactor. The control of the temperature at 40 °C was ensured by a double-heated  
83 jacket. The agitation rate varied, depending on the operating conditions used, as  
84 detailed in the results section. The digester operated in continuous-mode with a  
85 mean residence time of 28 days, which implied the supply of 3.5 L of cattle manure  
86 and removal of 3.5 L of digestate each day. Due to the viscosity of the liquid phase,  
87 two Archimede’s screw pumps (Air et Eau systèmes, Ludres, France) were used for  
88 supply and outlet. The supply was preliminary filtered using a grid with 6 mm  
89 diameter holes to prevent pipe plugging. Biogas composition and production were  
90 determined using dedicated on-line gas chromatography and gasmeter as previously  
91 described in Lebranchu et al. (2017).

## 92 *2.2. Dense membrane properties and characterization*

93 To avoid the presence of hydrogen in the biogas at the outlet of the reactor, which  
94 would require the introduction of a recirculation loop of the biogas, the hydrogen  
95 injection was not carried out by a conventional sparger but by permeation into a  
96 silicone tube pressurized by closing it at one end and wrapped around a cylindrical  
97 support. The silicone tube used was a membrane with 0.3 mm thickness and an  
98 internal diameter of 2 mm (Witeg, Wertheim, Germany). The permeability  $\mathcal{P}$  of the  
99 hydrogen in the silicone was obtained from equation 1 by applying various pressure  
100 gradients and measuring the related gas flow rate. The experiments were conducted

101 in air, water and digestate.

$$\mathcal{P} = \frac{Q \cdot e}{A \cdot \Delta P} \quad (1)$$

102 with  $\mathcal{P}$  ( $\text{m}^3 \text{ m}/(\text{s m}^2 \text{ Pa})$ ) the membrane permeability,  $Q$  the volumetric flow rate  
103 ( $\text{m}^3/\text{s}$ ),  $e$  the membrane thickness (m),  $A$  the membrane surface ( $\text{m}^2$ ) and  $\Delta P$  (Pa)  
104 the pressure difference. In order to enhance liquid circulation in the core of the vessel,  
105 the diameter of the membrane support was increased to a maximal value of 324 mm.  
106 A gap of 65 mm was left between the top of the scraper placed on the stirrer and the  
107 bottom of the wrapping of the membrane tube to allow the circulation of the fluid.  
108 For the same reason, a gap of 65 mm was applied between the top of the membrane  
109 tube and the surface of the liquid. Using these conditions, a maximum of 100 m of  
110 membrane could be wrapped. According to the equation 1, the expected hydrogen  
111 flow rate **should** be 35 mL/min approximately.

112 The hydrogen flow rates and the volumetric gas-liquid mass transfer coefficients  
113  $k_L a$  of the set-up were also determined. Gas-liquid mass transfer measurements  
114 were carried-out by setting the permeation rate at the inlet of the membrane and  
115 measuring the pressure inside the membrane tube. Dissolved  $\text{H}_2$  was obtained from  
116 the mass balance between the inlet and the outlet. The experiment was carried-out  
117 as follows : The reactor was filled with 100 L of water heated gradually to 40 °C for  
118 12 hours. Before the start of the measurements, a purge of the membrane tube was  
119 done at 20 mL / min of  $\text{H}_2$  for 20 min in order to remove the gases that could be  
120 introduced inside the tube. The end of the tube was then closed and the flow rate  
121 studied was fixed to the flow meter. Continuous hydrogen injections were made in  
122 water at 10, 30 and 50 mL / min and, by the plot of equation 2,  $k_L a$  ( $\text{s}^{-1}$ ) value was  
123 then obtained.

$$\ln \left( \frac{[H_2]^*}{[H_2]^* - [H_2]} \right) = k_L a \cdot t \quad (2)$$

124 with  $[H_2]^*$  the concentration of  $H_2$  at saturation,  $[H_2]$  the concentration of  $H_2$  in  
 125 the solution and  $t$  the time (s).

### 126 3. Results and discussion

#### 127 3.1. Gas-liquid mass transfer

128 The permeability of hydrogen in the silicone was determined at 40°C using sev-  
 129 eral injection rates (30, 50 and 70 mL / min) and considering permeation in air to  
 130 neglect the resistance of mass transfer in the fluid phase (Figure 2). A value of  $\mathcal{P}$   
 131 =  $7.33 \times 10^{-14}$  (m<sup>3</sup> m) / (s m<sup>2</sup> Pa) was obtained. As expected, the increase of the  
 132 resistance of mass transfer entailed a slower permeation of hydrogen in water and in  
 133 digestate due to the significant increase of the resistance to mass transfer when air is  
 134 replaced by these two fluids (Figure 2). In parallel, the determination of  $k_L a$  values,  
 135 carried-out at a agitation rate of 10 rpm (namely for a constant power dissipation per  
 136 unit of volume) provided values of approximately 1 h<sup>-1</sup> (Figure 2). No study deter-  
 137 mining the value of  $k_L a$  of a dense membrane for hydrogen injection in digesters have  
 138 been carried out at the pilot-scale making hard the comparison of **the present** values  
 139 with literature data. An increase of the agitation rate to 40 rpm did not promote an  
 140 increase in the hydrogen absorption rate as  $H_2$  microbubbles, formed and attached  
 141 to the membrane, detached then due to higher local shear stress, causing a sudden  
 142 release of gaseous  $H_2$  and then a decrease in the amount of dissolved hydrogen.

#### 143 3.2. Validation of pilot-scale digester

144 The biogas flowrate profile showed that, after 17 days of production, it reached  
 145 an asymptotic value of about 5.2 NL/h (or 1 NL/(h kg<sub>OM</sub>)), which corresponded to

146 a production of 125 L of biogas per day. Considering the daily addition of 3.5 L of  
147 liquid cattle manure, at a rate of about 11 % of organic matter, biogas production  
148 was approximately 324 L/kg<sub>OM</sub>. This result was thus in agreement with the expected  
149 values of biogas production using cattle manure (Teixeira Franco et al., 2017). The  
150 initial pH was 7.9, corresponding to the pH of the digestate used for initial reactor  
151 filling. During the first 7 days of digestion, a slight pH decrease was observed before  
152 a stabilization to 7.5 after 20 days of digestion, which corresponded to range of values  
153 of 7.5 to 8, typically encountered in digesters (Bassani et al., 2015).  
154 The analysis of biogas composition revealed a maximal methane content of 63.6 %  
155 and a minimal CO<sub>2</sub> rate of 36.3 % after 3 days of digestion. This initial process  
156 sequence, rather favourable to methane production was already noticed in differ-  
157 ent metagenomic studies such as the works of Montero et al. (2008) on a synthetic  
158 medium or of Chachkhiani et al. (2004) using liquid cattle manure. This suggested  
159 thus an initial production of CH<sub>4</sub> by the hydrogenotrophic *Archae* rather than by  
160 the acetotrophic populations leading to the reduction of CO<sub>2</sub>. Biogas composition  
161 progressively stabilized after 7 days of digestion at rate values of 57.7 % for CH<sub>4</sub>  
162 and 42 % for CO<sub>2</sub>. The results obtained without hydrogen injection thus validated  
163 the pilot-scale digester as a scale-up of the equipment used by Lebranchu et al.  
164 (2017) for cattle manure methanization and could thus be used for further study of  
165 biomethanation process.

### 166 3.3. *In-situ biomethanation*

#### 167 3.3.1. *Impact of H<sub>2</sub> flowrate on biogas flowrate*

168 After each steady-state, H<sub>2</sub> flow rate was progressively increased from 12 to 31  
169 mL/min. Biogas flow rate per kg of organic matter was determined and given in Fig-  
170 ure 3A. Hydrogen injection, whatever the flowrate used, did not seem to significantly

171 modify biogas flowrate. This was previously observed by Luo et al. (2012) by increas-  
172 ing partial pressure of H<sub>2</sub> in a digester headspace. This result was also consistent  
173 with the bioreaction stoichiometry as one molecule of CO<sub>2</sub> should be transformed  
174 into one molecule of methane. This also meant that all injected hydrogen was ef-  
175 fectively consumed. As the consumption of exogenous H<sub>2</sub> led to the consumption  
176 of a fraction of the dissolved CO<sub>2</sub>, there was also a concomitant slight increase in  
177 the pH value after each increase of hydrogen flowrate (Figure 3B), from 7.5 to al-  
178 most 7.7 for H<sub>2</sub> flow rate of 31 mL/min. However, this increase, also observed in  
179 other studies of biological methanation (Szuhaj et al., 2016; Luo et al., 2012; Luo  
180 and Angelidaki, 2013a), remained weak and did not seem to significantly affect the  
181 production process as the flow rate of biogas remained overall constant (Figure 3A).

### 182 3.3.2. Impact of H<sub>2</sub> flowrate on biogas composition

183 On the contrary to biogas flow rate, CH<sub>4</sub> and CO<sub>2</sub> biogas contents significantly  
184 depended on the H<sub>2</sub> flowrate as indicated by the measurements reported in Figure  
185 3A. A progressive decrease in CO<sub>2</sub> content and a corresponding increase in CH<sub>4</sub> con-  
186 tent were indeed observed when H<sub>2</sub> flowrate increased. Figure 3A also shows that, in  
187 the mean time, the time interval between change in H<sub>2</sub> flow rate and biogas content  
188 stabilization was reduced. Whereas five days were needed to achieve the stabiliza-  
189 tion after switching the H<sub>2</sub> flowrate from 0 to 12 mL/min, three days were indeed  
190 sufficient to achieve stability after the switch from 20 to 31 mL/min. This suggested  
191 a possible adaptation of microbial populations to the presence of H<sub>2</sub>, including the  
192 increase in the hydrogenotrophic bacteria population, promoting a reduction of the  
193 necessary stabilization time. Studies of Agneessens et al. (2017), Treu et al. (2018),  
194 and Alfaro et al. (2018, 2019) demonstrated by microbial community characterization  
195 that microbial populations were able to adapt to a H<sub>2</sub> injection but also that this

196 adaptation was strongly linked to the process operation parameters (modes of injection of H<sub>2</sub>, flow rates, substrates, reactor scale). The relationships between CH<sub>4</sub> and CO<sub>2</sub> contents and injected H<sub>2</sub> flowrates were reported in Figure 4. Interestingly, the experimental measurements could be fitted using a linear model which was expected regarding reaction stoichiometry. Considering that the molar volume remained indeed the same whatever the gas, a mole of CH<sub>4</sub> should be produced for each mole of CO<sub>2</sub> consumed. Knowing that the flow of biogas is 5.2 L/h, the slope obtained of 0.35 corresponded to 0.3 mL/min of additional CH<sub>4</sub> for 1 mL/min H<sub>2</sub> added. However, theoretically, with the addition of 1 mL/min of H<sub>2</sub>, the CH<sub>4</sub> flowrate should be of 0.25 mL/min. This clearly confirmed the efficiency of conversion of hydrogen into methane and that the injected hydrogen was completely consumed. This also suggested that consumed hydrogen seemed not significantly used for biomass growth, as Díaz et al. (2015) already showed. The total consumption of hydrogen was confirmed by the analysis of biogas with H<sub>2</sub> rates lower than 0.05 % (Figure 3A) despite weak amounts of H<sub>2</sub> of approximately 0.04 % at an hydrogen flowrate of 31 mL/min were determined. The simultaneous presence of CO<sub>2</sub> at high volume fractions also seemed to indicate the occurrence of local H<sub>2</sub> saturations in the bioreactor inducing a release of gaseous hydrogen. This may be explained either (i) by a physical limitation, namely the injected hydrogen was not dispersed quickly enough in the reactor in comparison with the inlet flowrate of hydrogen, leading to local saturation and the appearance of a gas phase hydrogen or (ii) by a biological limitation, namely *Archae* were not locally able to consume all the amount of injected hydrogen or (iii) by a local limitation of CO<sub>2</sub> that stopped the H<sub>2</sub> consumption. Even if biogas recirculation is an interesting option to limit H<sub>2</sub> loss, further developments regarding efficiency of 'one-pass' hydrogen injection, namely without biogas recirculation, should be intensified. Jensen et al. (2018) indeed demonstrated that

222 it should remain the optimal solution from a mass transfer performance point of view.

223

### 224 3.4. Impact of shear stress on biogas production during biomethanation

225 As noted previously, when the hydrogen flow rate and the agitation rate were  
226 respectively 31 mL/min and 10 rpm, traces of H<sub>2</sub> were measured at the outlet of  
227 the reactor. Thus, the frequency of agitation was modified in order to improve the  
228 distribution of hydrogen in the reactor and potentially to reduce this loss and to  
229 increase the CH<sub>4</sub> rate. The study of the impact of agitation rate was therefore  
230 performed here in the presence of an injection of H<sub>2</sub> to 31 mL/min.

#### 231 3.4.1. Impact on biogas flowrate

232 The temporal evolution of the flowrate of biogas for different conditions of agita-  
233 tion is presented in Figure 5. The increase in the agitation rate from 10 to 20 rpm  
234 did not have a significant impact on the flowrate of biogas. However, the reduction  
235 of agitation from 20 to 5 rpm led to an increase in the average flow rate from 0.89  
236 to 1.14 L/(h kg<sub>OM</sub>), but also to temporal fluctuations of this flow rate. This could  
237 be related to the results of previous paper dealing with the impact of agitation on  
238 the performance on biogas production in a 2 L digester (Lebranchu et al., 2017). It  
239 was indeed shown that the increase in agitation from 10 to 50 and 90 rpm, led to a  
240 reduction of the amount of biogas, probably due to the increase in the maximum in  
241 shear stress the reactor and the resulting damage of microbial aggregates. As shown  
242 by Lebranchu et al. (2017), this shear stress could be expressed by equation 3:

$$\sigma = K \cdot \dot{\gamma}^n \quad (3)$$

243 with  $K$  (Pa s<sup>*n*</sup>) the consistency index and  $n$  ( ) the flow index for the cattle manure  
 244 digestate. Then the following equation may also be obtained:

$$\frac{\sigma_{max100L}}{\sigma_{max2L}} \propto \left( \frac{\dot{\gamma}_{max100L}}{\dot{\gamma}_{max2L}} \right)^n \quad (4)$$

245 with  $\sigma_{max100L}$  and  $\sigma_{max2L}$  (Pa) and  $\dot{\gamma}_{max100L}$  et  $\dot{\gamma}_{max2L}$  the maximal shear stresses  
 246 and maximal shear rates in both systems respectively. Assuming that maximal shear  
 247 rate  $\dot{\gamma}_{max}$  was encountered in the gap between the ribbon and the vessel wall, it could  
 248 be estimated by equation 5.

$$\dot{\gamma}_{max} = \frac{\pi \cdot N \cdot D}{\frac{D_{vessel} - D}{2}} \quad (5)$$

249 with  $D_{vessel}$  the vessel diameter,  $D$  the external ribbon diameter and  $N$  the agitation  
 250 rate. The width of the gap in the 100 L reactor was also decreased relatively to its  
 251 length obtained theoretically by geometric similarity of the 2L reactor in order to  
 252 increase the heat transfer and limit the formation of crust close to the outer wall.  
 253 Thus, the maximal shear rate reached 12.6 s<sup>-1</sup> in 100 L reactor at 5 rpm, which is  
 254 2 times higher than the one obtained in the 2 L reactor at 10 rpm (6.1 s<sup>-1</sup>). The  
 255 maximal shear stress obtained at 10 rpm in 2 L reactor was about 30 Pa (Lebranchu  
 256 et al., 2017), so according to equation 4, the maximal shear stress obtained at 5 rpm  
 257 in the pilot reactor was 37.2 Pa. Using the same method of calculation, the maximal  
 258 shear stress at the pilot-scale and at an agitation rate of 10 rpm was then estimated  
 259 at  $\sigma_{max} = 47$  Pa. Thus, the maxim shear stress in 2 L at  $N = 10$  rpm was similar  
 260 to the one expected in the 100 L digester for  $N = 5$  rpm, and matched the critical  
 261 shear stress that should not be exceeded, as determined in Lebranchu et al. (2017).  
 262 During the experiment at  $N = 10$  rpm in the 100 L reactor, the maximal stress was

263 thus high enough to lead to a reduction of the biogas flowrate.  
264 Moreover, the variability of the flow rate was more important at an agitation rate  
265 of 5 rpm in comparison with 10 or 20 rpm agitations. This phenomenon found no  
266 explanation by the measurements and no high frequency fluctuations could be put  
267 into evidence. The change in the frequency of agitation did not significantly change  
268 the pH of the digestate (data not shown). The relative stability of the pH during  
269 this period indicated that the balance between the production and consumption of  
270 volatile fatty acids was globally not impacted by the agitation rate. The biogas  
271 flow variations observed at  $N = 5$  rpm could therefore not be explained by pH  
272 fluctuations.

#### 273 *3.4.2. Impact on biogas composition*

274 The evolution of the composition in  $\text{CH}_4$  and  $\text{CO}_2$  flowrates for the various agi-  
275 tation rates (10, 20 and 5 rpm) **was** reported in Figure 5. The increase in agitation  
276 from 10 to 20 rpm allowed an increase in  $\text{CH}_4$  rate from 68.0 to 68.8 %, a decrease in  
277  $\text{CO}_2$  rate from 31.7 to 30.9 % and a residual  $\text{H}_2$  rate reduction from 0.041 to 0.034  
278 %. This suggested that a stronger agitation allowed a better homogeneity of the  $\text{H}_2$   
279 and thus a more efficient consumption. The change from  $N = 20$  to 5 rpm led **also** to  
280 biogas composition fluctuations. This destabilization was accompanied by a decrease  
281 in the average  $\text{CH}_4$  rate to 66.7 %, an increase in the  $\text{CO}_2$  rate to 33.1 % and an  
282 increase in the  $\text{H}_2$  rate to 0.08 %. Considering the respective flow rates of each gas  
283 component, a slight increase in hydrogen flow rate of 1 mL/h at 20 rpm versus 3  
284 mL/h to 5 rpm, which seemed to indicate to a slight decline in methane flow rate,  
285 but  $\text{CH}_4$  flow rate increased from 3.03 to 3.5 L/h. Thus, the hydrogen mass balance  
286 was not in total agreement with the one in methane, with a simultaneous increase  
287 in the flow of methane and hydrogen. These results suggested that the additional

288 methane produced was not related to the injection of hydrogen but could be the  
289 consequence of better syntrophic relationships between bacteria as it was already  
290 suggested in the study of Lebranchu et al. (2017). Thus, it was concluded that the  
291 increase in agitation allowed a better distribution of hydrogen in the reactor, pro-  
292 moted a reduction in H<sub>2</sub> rate in biogas, but also caused a decrease in overall biogas  
293 production flow. The agitation was then set back to 10 rpm for the rest of the study.

### 294 3.5. Addition of exogenous CO<sub>2</sub>

295 To further validate the hypothesis of local CO<sub>2</sub> limitation, CO<sub>2</sub> was added in the  
296 injected gas, by applying the ratio of H<sub>2</sub> and total C carbon rates  $H_2/C = 8.8$ . This  
297 addition was carried-out in 2 steps. First, the addition of CO<sub>2</sub> was made at a flow  
298 rate of 3.5 mL/min, while maintaining the flow of H<sub>2</sub> at 31 mL/min. In a second  
299 step, the flow rate of CO<sub>2</sub> was maintained constant at 3.5 mL/min while H<sub>2</sub> flow  
300 rate was increased till total consumption of injected CO<sub>2</sub>. The Figure 6 reports the  
301 total flow rate of biogas at the outlet of the digester. A slight increase in this flow  
302 rate was observed throughout the period of CO<sub>2</sub> injection, from 5.0 L/h to 5.6 L/h.  
303 The observed increase of the overall flow rate was consistent with what was expected,  
304 although this increase was three times higher than the expected value for a CO<sub>2</sub> inlet  
305 flow rate of 0.21 L/h. Besides, no decrease of pH during the addition of CO<sub>2</sub> was  
306 observed meaning there was no accumulation of CO<sub>2</sub> in the reactor. This suggested  
307 that dissolved CO<sub>2</sub> remained close to the permeation membrane, and that it was  
308 either consumed, or accumulated before its stripping. This would suggest a local  
309 decrease of the pH, close to the membrane, as previously demonstrated by Garcia-  
310 Robledo et al. (2016). Lastly, the increase of H<sub>2</sub> flow rate led to a slight increase  
311 in the pH measured, from 7.7 to 7.8, which was consistent with the consumption of  
312 CO<sub>2</sub> naturally formed by the digestion process.

313

314 The injection of CO<sub>2</sub> at 3.5 mL/min with a H<sub>2</sub> flow rate of hydrogen set at 31  
315 mL/min led to an increase in the rate of CO<sub>2</sub> in biogas and, consequently, a decrease  
316 in CH<sub>4</sub> rate (Figure 6). Combined with the overall increase in the flow of biogas, this  
317 increase in CO<sub>2</sub> rate led to the increase in CO<sub>2</sub> outflow from 1.66 to 1.94 L/h, while  
318 CO<sub>2</sub> injected was 0.21 L/h, indicating an overproduction of CO<sub>2</sub> in these conditions.  
319 Figure 6 shows that the amount of CO<sub>2</sub> consumed is not zero because the present rate  
320 of H<sub>2</sub> in the biogas decreased in the presence of CO<sub>2</sub>. Concerning H<sub>2</sub>, its rate fell from  
321 0.16 to 0.008 %, meaning its flow rate decreased from 0.13 to 0.0083 mL/min. At the  
322 same time, methane rate was reduced from 66.7 to 65.1 %, but the increase in overall  
323 throughput of biogas led to an increase in the overall rate of methane from 3.34 to  
324 3.66 L/h. The increased flow rate of methane is qualitatively consistent with the  
325 decrease in the rate of hydrogen. Quantitatively, the simultaneous overproduction of  
326 CO<sub>2</sub> and CH<sub>4</sub> could be explained by the acetotrophic *Archae* that produce both of  
327 CH<sub>4</sub> and CO<sub>2</sub>. The local decrease in pH mentioned earlier would be the consequence  
328 of the activity of the acetotrophic *Archae*. This phenomenon was demonstrated by  
329 the study of Hao et al. (2013) who observed changes in bacterial populations during  
330 changes of pH conditions. It has been highlighted that the increase in the pH above  
331 7.5 led to an inhibition of the activity of the acetotrophic methanogenic *Archae* .  
332 Thus, considering the initial pH of 7.8 in the whole of the reactor, the addition of  
333 CO<sub>2</sub> could have led to a local decrease in pH below 7.5, which would cause the over-  
334 production of methane and CO<sub>2</sub>. Thus, it seems that, qualitatively, the depletion of  
335 H<sub>2</sub> in the outlet gas was explained by consumption of a fraction of CO<sub>2</sub>. However,  
336 it remained difficult to quantify it more precisely due to the increased production of  
337 CO<sub>2</sub> by acetotrophic *Archae* .

338 The addition of extra CO<sub>2</sub> mixed with the H<sub>2</sub> allowed the total consumption of

339 the H<sub>2</sub> (Figure 6). This could explain why hydrogen was detected in outlet biogas  
340 for flow injection of 31 mL/min of pure hydrogen, even if CO<sub>2</sub> was macroscopically  
341 available. The study of Garcia-Robledo et al. (2016) showed that injected H<sub>2</sub> and  
342 CO<sub>2</sub> consumption was carried out in a millimetric layer near the membrane. This  
343 suggested that, in the absence of CO<sub>2</sub> injected, the existence of residual hydrogen  
344 was due to a CO<sub>2</sub> limitation near the membrane. A realistic assumption is that the  
345 injected H<sub>2</sub> locally reacted with CO<sub>2</sub> which, once the latter fully consumed, caused  
346 a local accumulation of hydrogen beyond its solubility, entailing its stripping. So,  
347 there was probably a limitation of hydrogen transport from the membrane towards  
348 the rest of the reactor and a limitation on the transport of CO<sub>2</sub> from bulk to the  
349 membrane permeation vicinity. This assumption was also previously proposed by  
350 Garcia-Robledo et al. (2016) and Agneessens et al. (2018) in 1.4 L lab-scale digesters.

351

352 In order to consume the injected CO<sub>2</sub>, H<sub>2</sub> flow rate was progressively increased  
353 while keeping constant the CO<sub>2</sub> flow rate to 3.5 mL/min. It should be noted that it  
354 was necessary to increase the H<sub>2</sub> flow rate up to 42 mL/min (Figure 6) to achieve  
355 a CO<sub>2</sub> rate in the biogas similar to the rate of CO<sub>2</sub> with pure H<sub>2</sub> injection, i.e. to  
356 consume all of the exogenous CO<sub>2</sub>. Even if the increase in total production of biogas  
357 was explained by overproduction by the acetotrophic *Archae*, this consumption of  
358 additional hydrogen showed that the hydrogenotrophic *Archae* were always present  
359 and active. Flow rate of biogas was stable at 5.6 L/h over the period, but the flow  
360 rate of methane increased up to 3.8 L/h and that of CO<sub>2</sub> decreased to 1.8 L/h. The  
361 difference was thus + 0.14 L/h in CH<sub>4</sub> and - 0.14 L/h in CO<sub>2</sub>. The surplus of added  
362 hydrogen was thus 0.66 L/h, while the theoretical value was 0.17 L/h of additional  
363 methane and 0.17 L/h for CO<sub>2</sub> consumption. The results obtained in the digester  
364 were therefore relatively close to the theoretical values. Throughout this period,

365 the injected  $H_2$  was completely consumed, which confirmed the effectiveness of the  
366 permeation membrane for the intensification of production as long as it remained  
367 some  $CO_2$  to consume in the membrane vicinity.

368 Lastly, the injection of  $CO_2$  was shut-off, which led to the decrease in the flow of  
369 biogas from 5.6 to 5.0 L/h (Figure 6), to the increase in  $CH_4$  rate to 70.5 %, to  
370 the decrease in  $CO_2$  rate at 28.9 % and the measurement of about 0.4 %  $H_2$  in the  
371 biogas. The presence of hydrogen in the biogas while keeping a  $CO_2$  rate of nearly 30  
372 % indicated the appearance of a local saturation, likely located in the environment  
373 of the membrane.

#### 374 4. Conclusion

375 Biomethanation of cattle manure was validated in a 100 L digester using a dense  
376 membrane for  $H_2$  injection. This injection was shown to strongly limit the undis-  
377 solved  $H_2$  rate in the biogas produced. A linear relationship was found between the  
378  $CH_4$  content in the biogas and the  $H_2$  flowrate. The co-injection of exogenous  $CO_2$   
379 with  $H_2$  revealed that biogas production was probably limited by the dissolved  $CO_2$   
380 transport within the liquid phase volume, which addresses the issue of the definition  
381 of robust scale-up rules for biomethanation processes and for designs of gas injection  
382 systems.

#### 383 Acknowledgements

384 This work was supported by ADEME and Programme d'Investissements d'Avenir  
385 (research program VALORCO).

386 **References**

- 387 1. Agneessens, L. M., Ottosen, L. D. M., Andersen, M., Olesen, C. B., Feilberg,  
388 A., Kofoed, M. V. W., 2018. Parameters affecting acetate concentrations dur-  
389 ing in-situ biological hydrogen methanation. *Bioresource Technol.* 258, 33-40.
- 390 2. Agneessens, L. M., Ottosen, L. D. M., Voigt, N. V., Nielsen, J. L., de Jonge, N.,  
391 Fischer, C. H., Kofoed, M. V. W., 2017. In-situ biogas upgrading with pulse H<sub>2</sub>  
392 additions: The relevance of methanogen adaption and inorganic carbon level.  
393 *Bioresource Technol.* 233, 256-263.
- 394 3. Alfaro, N., Fdz-Polanco, M., Fdz-Polanco, F., Diaz, I., 2018. Evaluation of  
395 process performance, energy consumption and microbiota characterization in  
396 a ceramic membrane bioreactor for ex-situ biomethanation of H<sub>2</sub> and CO<sub>2</sub>.  
397 *Bioresource Technol.* 258, 142-150.
- 398 4. Alfaro, N., Fdz-Polanco, M., Fdz-Polanco, F., Diaz, I., 2019. H<sub>2</sub> addition  
399 through a submerged membrane for in-situ biogas upgrading in the anaerobic  
400 digestion of sewage sludge. *Bioresource Technol.* 280, 1-8.
- 401 5. Bassani, I., Kougiass, P. G., Treu, L., Angelidaki, I., 2015. Biogas upgrading via  
402 hydrogenotrophic methanogenesis in two-stage continuous stirred tank reactors  
403 at mesophilic and thermophilic conditions. *Environ. Sci. Technol.* 49, 12585-  
404 12593.
- 405 6. Chachkhiani, M., Dabert, P., Abzianidze, T., Partskhaladze, G., Tsiklauri, L.,  
406 Dudaauri, T., Godon, J., 2004. 16s rDNA characterisation of bacterial and  
407 archaeal communities during start-up of anaerobic thermophilic digestion of  
408 cattle manure. *Bioresource Technol.* 93, 227-232.
- 409 7. Diaz, I., Perez, C., Alfaro, N., Fdz-Polanco, F., 2015. A feasibility study on the  
410 bioconversion of CO<sub>2</sub> and H<sub>2</sub> to biomethane by gas sparging through polymeric

- 411 membranes. *Bioresource Technol.* 185, 246-253.
- 412 8. Garcia-Robledo, E., Ottosen, L. D., Voigt, N. V., Kofoed, M., Revsbech, N.  
413 P., 2016. Micro-scale H<sub>2</sub>-CO<sub>2</sub> dynamics in a hydrogenotrophic methanogenic  
414 membrane reactor. *Frontiers in Microbiol.* 7, 1276.
- 415 9. Hao, L., Lu, F., Li, L., Wu, Q., Shao, L., He, P., 2013. Self-adaption of  
416 methaneproducing communities to pH disturbance at different acetate concen-  
417 trations by shifting pathways and population interaction. *Bioresource Technol.*  
418 140, 319-327.
- 419 10. Jensen, M. B., Kofoed, M. V. W., Fischer, K., Voigt, N. V., Agneessens, L.  
420 M., Batstone, D. J., Ottosen, L. D. M., 2018. Venturi-type injection system as  
421 a potential H<sub>2</sub> mass transfer technology for full-scale in situ biomethanation.  
422 *Appl. Energ.* 222, 840-846.
- 423 11. Ju, D.-H., Shin, J.-H., Lee, H.-K., Kong, S.-H., Kim, J.-I., Sang, B.-I., 2008. Ef-  
424 fects of pH conditions on the biological conversion of carbon dioxide to methane  
425 in a hollow-fiber membrane biofilm reactor (Hf-MBfR). *Desalination* 234, 409-  
426 415.
- 427 12. Kim, S., Choi, K., Chung, J., 2013. Reduction in carbon dioxide and pro-  
428 duction of methane by biological reaction in the electronics industry. *Int. J.*  
429 *Hydrogen Energ.* 38, 3488-3496.
- 430 13. Kougiyas, P. G., Treu, L., Benavente, D. P., Boe, K., Campanaro, S., Angeli-  
431 daki, I., 2017. Ex-situ biogas upgrading and enhancement in different reactor  
432 systems. *Bioresource Technol.* 225, 429-437.
- 433 14. Lebranchu, A., Delaunay, S., Marchal, P., Blanchard, F., Pacaud, S., Fick, M.,  
434 Olmos, E., 2017. Impact of shear stress and impeller design on the production  
435 of biogas in anaerobic digesters. *Bioresource Technol.* 245, 1139-1147.
- 436 15. Luo, G., Angelidaki, I., 2012. Integrated biogas upgrading and hydrogen uti-

- 437            lization in an anaerobic reactor containing enriched hydrogenotrophic methanogenic  
438            culture. *Biotechnol. Bioeng.* 109, 2729-2736.
- 439    16. Luo, G., Angelidaki, I., 2013a. Co-digestion of manure and whey for in situ  
440            biogas upgrading by the addition of H<sub>2</sub>: Process performance and microbial  
441            insights. *Applied Microbiol. Biot.* 97, 1373-1381.
- 442    17. Luo, G., Angelidaki, I., 2013b. Hollow -fiber membrane based H<sub>2</sub> diffusion for  
443            efficient in situ biogas upgrading in an anaerobic reactor. *Appli. Microbiol.*  
444            *Biot.* 97, 3739-3744.
- 445    18. Luo, G., Johansson, S., Boe, K., Xie, L., Zhou, Q., Angelidaki, I., 2012a.  
446            Simultaneous hydrogen utilization and in situ biogas upgrading in an anaerobic  
447            reactor. *Biotechnol. Bioeng.* 109, 1088-1094.
- 448    19. Luo, G., Johansson, S., Boe, K., Xie, L., Zhou, Q., Angelidaki, I., 2012b.  
449            Simultaneous hydrogen utilization and in situ biogas upgrading in an anaerobic  
450            reactor. *Biotechnol. Bioeng.* 109, 1088-1094.
- 451    20. Montero, B., Garcia-Morales, J., Sales, D., Solera, R., 2008. Evolution of  
452            microorganisms in thermophilic-dry anaerobic digestion. *Bioresource Technol.*  
453            99, 3233-3243.
- 454    21. Szuhaj, M., Acs, N., Tengolics, R., Bodor, A., Rakhely, G., Kovacs, K. L.,  
455            Bagi, Z., 2016. Conversion of H<sub>2</sub> and CO<sub>2</sub> to CH<sub>4</sub> and acetate in fed-batch  
456            biogas reactors by mixed biogas community: a novel route for the power-to-gas  
457            concept. *Biotechnol. Biofuels* 9, 102.
- 458    22. Texeira Franco, R., Buffiere, P., Bayard, R., 2017. Cattle manure for biogas  
459            production. Does ensiling and wheat straw addition enhance preservation of  
460            biomass and methane potential? *Biofuels*, 1-12.
- 461    23. Treu, L., Kougias, P. G., de Diego-Diaz, B., Campanaro, S., Bassani, I.,  
462            Fernandez-Rodriguez, J., and Angelidaki, I. 2018. Two-year microbial adap-

- 463 tation during hydrogen-mediated biogas upgrading process in a serial reactor  
464 configuration. *Bioresource Technol.* 264, 140-147.
- 465 24. Wang, W., Xie, L., Luo, G., Zhou, Q., Angelidaki, I., 2013. Performance  
466 and microbial community analysis of the anaerobic reactor with coke oven gas  
467 biomethanation and in situ biogas upgrading. *Bioresource Technol.* 146, 234-  
468 239.

469 **Figure captions**

470 **Figure 1.** Sketch of the bioreactor used in the present study.

471

472 **Figure 2.** Impact of transmembrane pressure on hydrogen permeation flow rate  
473 in the case of permeation in air (■), in water (▲) and in digestate (●) and on the  
474 volumetric gas-liquid mass transfer coefficient  $k_La$  in digestate (×).

475

476 **Figure 3.** (A) Temporal profile of biogas flowrate (□) and composition in CO<sub>2</sub>  
477 (◇), H<sub>2</sub> (\*) and CH<sub>4</sub> (○) and (B) pH.

478

479 **Figure 4.** Impact of H<sub>2</sub> flowrate on the rates of methane (○) and CO<sub>2</sub> (◇).

480

481 **Figure 5.** Impact of agitation rate on the total (□), CO<sub>2</sub> (◇), H<sub>2</sub> (\*) and CH<sub>4</sub>  
482 (○) volumetric flowrates.

483

484 **Figure 6.** Impact of CO<sub>2</sub>+H<sub>2</sub> injection on the CO<sub>2</sub> (◇), H<sub>2</sub> (\*) and CH<sub>4</sub> (○) biogas  
485 composition and total biogas volumetric flowrate (□) .

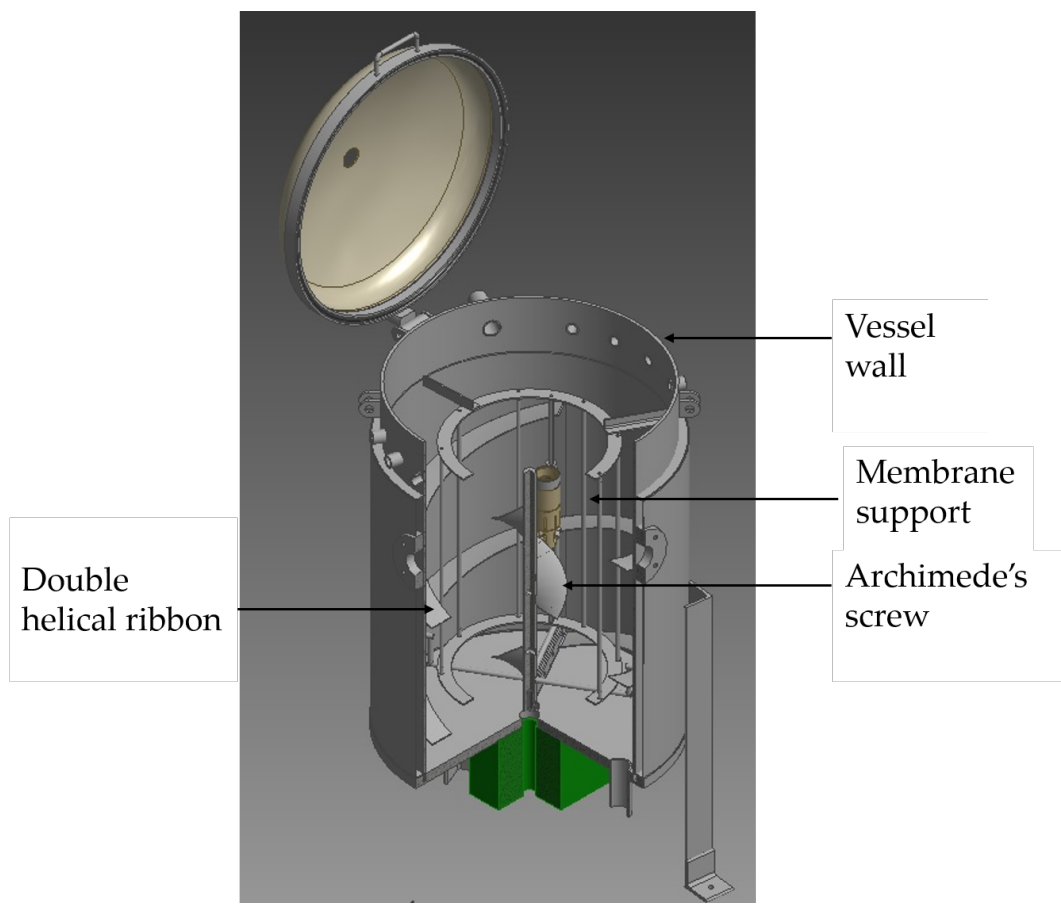


Figure 1: Sketch of the bioreactor used in the present study.

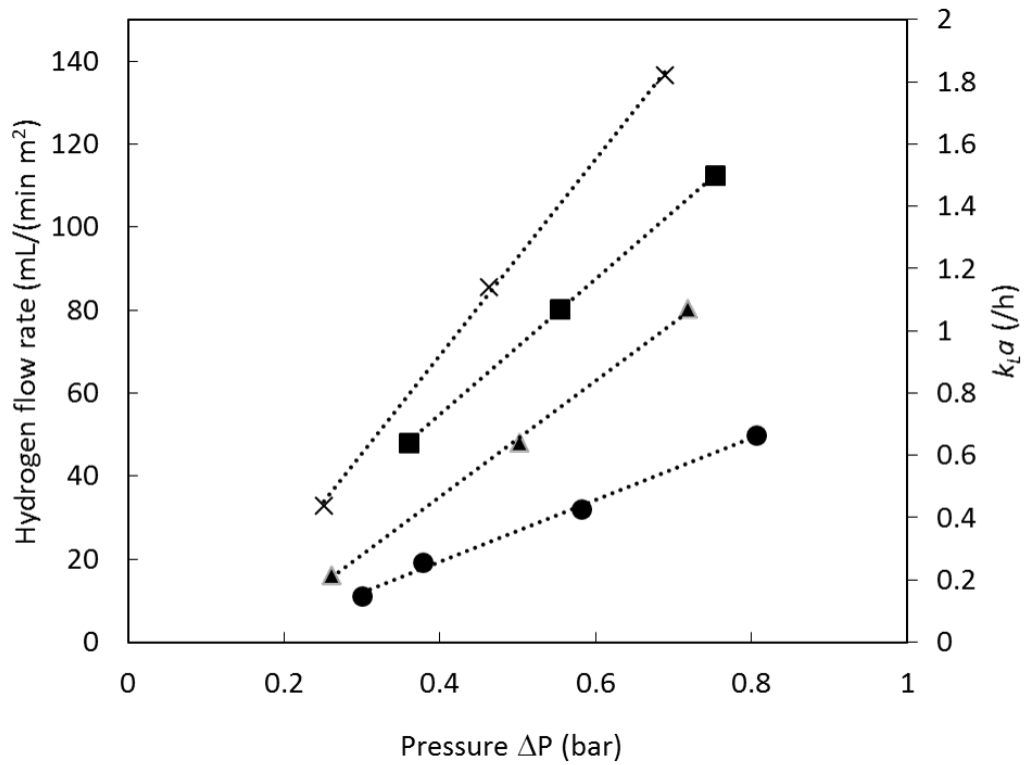
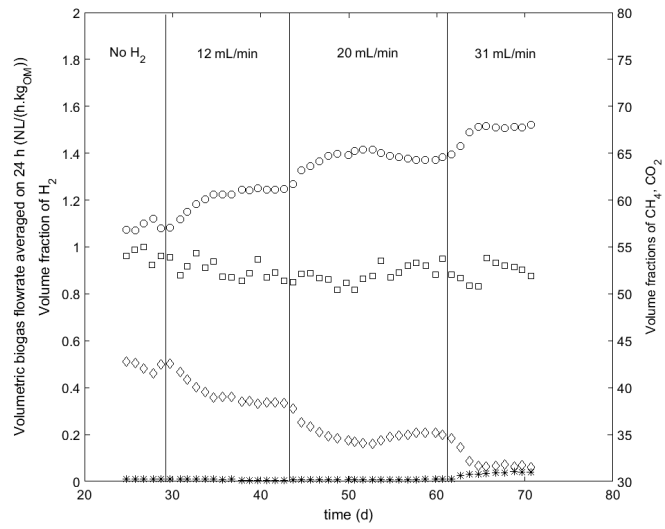
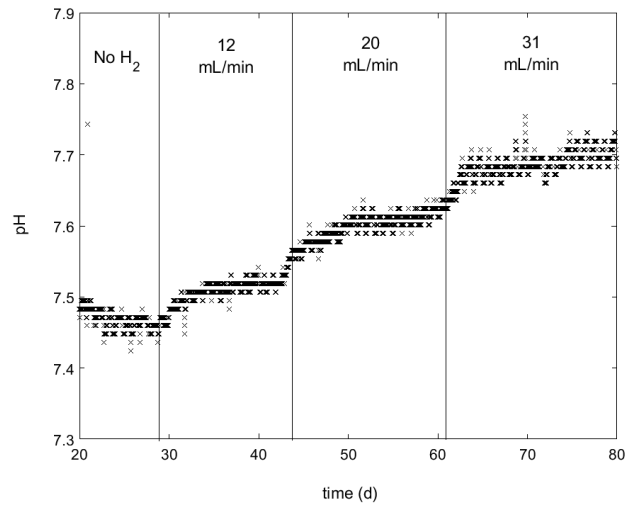


Figure 2: Impact of transmembrane pressure on hydrogen permeation flow rate in the case of permeation in air (■), in water (▲) and in digestate (●) and on the volumetric gas-liquid mass transfer coefficient  $k_{La}$  in digestate (×.)



(A)



(B)

Figure 3: (A) Temporal profile of biogas flowrate ( $\square$ ) and composition in  $\text{CO}_2$  ( $\diamond$ ),  $\text{H}_2$  ( $*$ ) and  $\text{CH}_4$  ( $\circ$ ) and (B) pH.

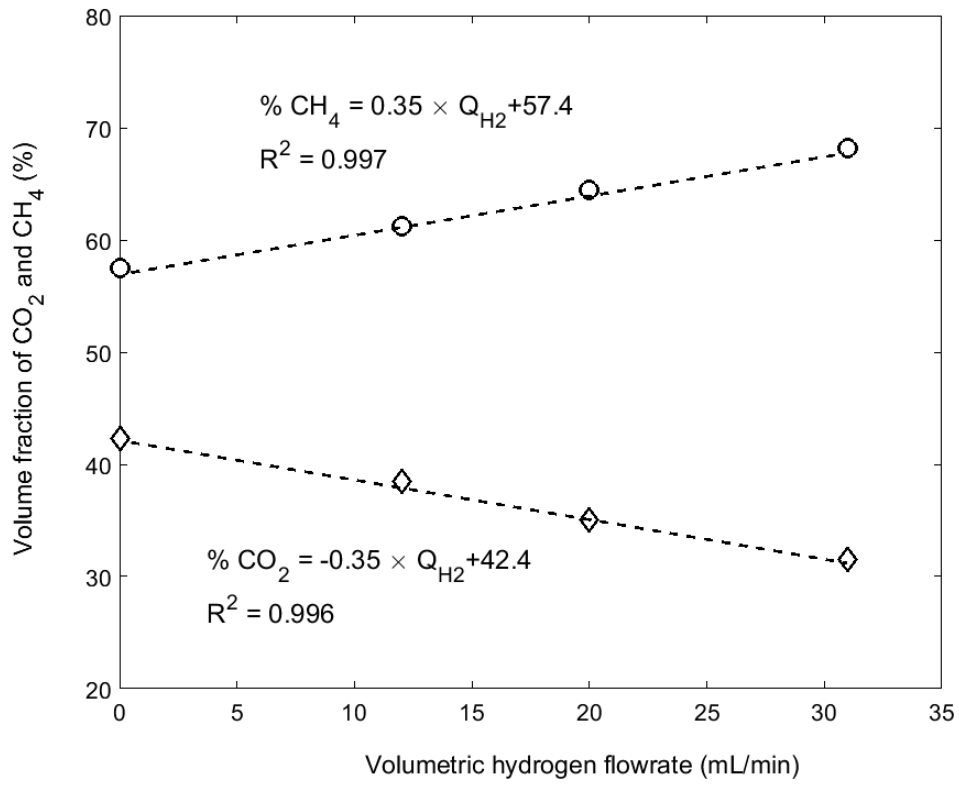


Figure 4: Impact of H<sub>2</sub> flowrate on the rates of methane in CO<sub>2</sub> (◇) and CH<sub>4</sub> (○) .

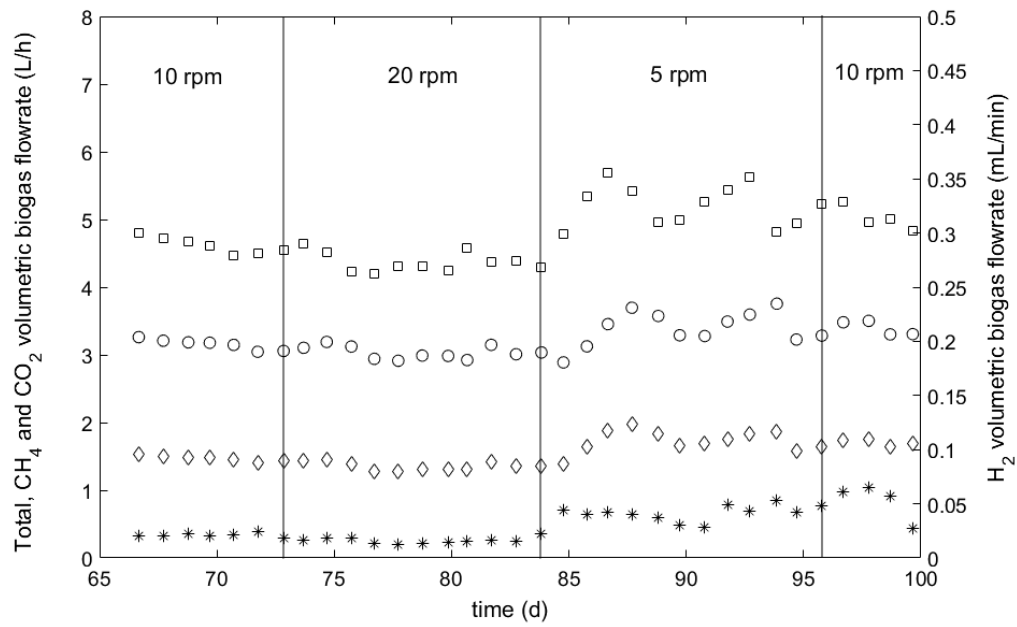


Figure 5: Impact of agitation rate on the total ( $\square$ ),  $\text{CO}_2$  ( $\diamond$ ),  $\text{H}_2$  ( $*$ ) and  $\text{CH}_4$  ( $\circ$ ) volumetric flowrates.

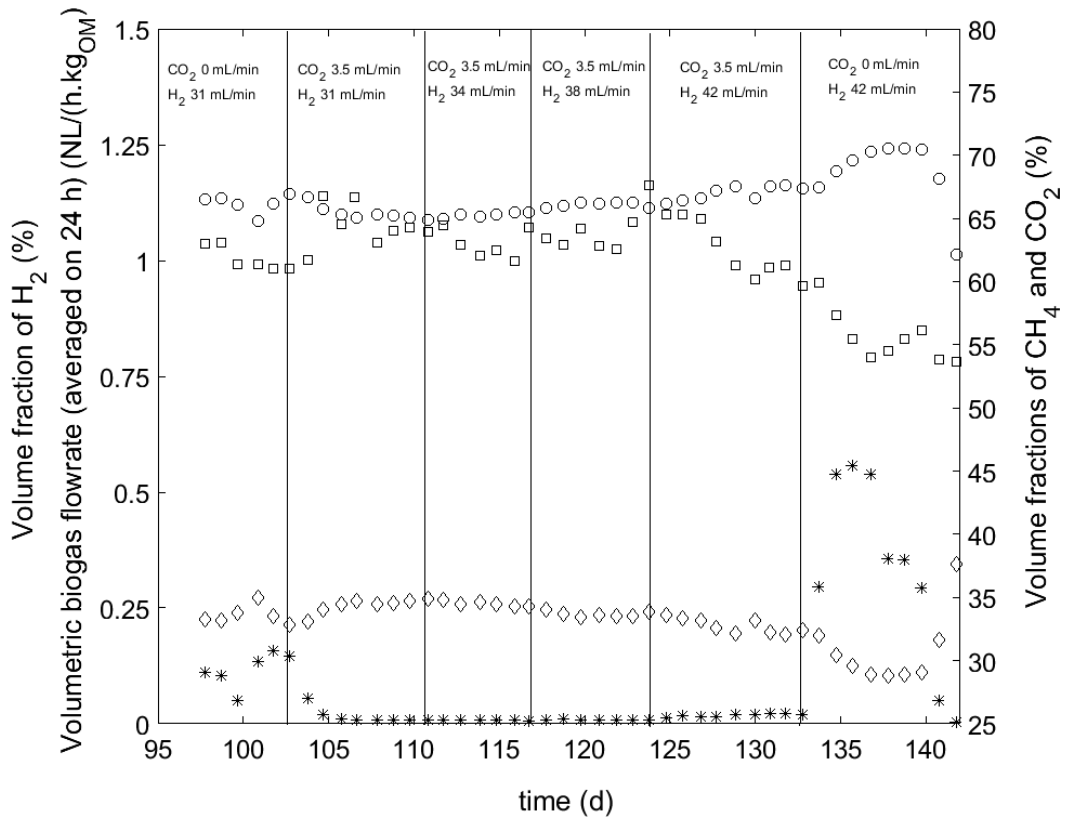


Figure 6: Impact of CO<sub>2</sub>+H<sub>2</sub> gas on the CO<sub>2</sub> (◇), H<sub>2</sub> (\*) and CH<sub>4</sub> (○) biogas composition and total biogas volumetric flowrate (□).